Applied Water Science (2018) 8:114
https://doi.org/10.1007/s13201-018-0755-1

ORIGINAL ARTICLE

The adsorption of $HCrO_4^-$ on activated carbon of date pits and its photoreduction on the hetero-system $ZnCo_2O_4/TiO_2$

Y. Azoudj[1,2] · Z. Merzougui[1] · G. Rekhila[3] · M. Trari[3]

Received: 29 January 2018 / Accepted: 17 June 2018 / Published online: 2 July 2018

Abstract

The adsorption properties of activated carbon were successfully tested toward the elimination of hazardous $HCrO_4^-$ (30, 50, 70 and 100 mg L^{-1}). The material was prepared from Algerian date pits by physical and chemical activations of $ZnCl_2$/CO_2 in the goal to develop the microporous volume. The characterization by N_2 adsorption at 77 K, the mercury intrusion porosimetry and scanning electron microscopy showed important textural properties. CO_2 increases the specific surface area (1192 m^2 g^{-1}) and pore volume (0.96 cm^3 g). The $HCrO_4^-$ adsorption is described by a pseudo-first-order kinetic model, and the equilibrium data are fitted by the Langmuir model with a maximal adsorption capacity of 46.72 mg/g within 30 min and a constant K_L (0.12 L g^{-1}). The remaining $HCrO_4^-$ concentrations (8, 23, 32.5 and 43.5 mg L^{-1}) were photocatalytically reduced on the hetero-system $ZnCo_2O_4/TiO_2$ down to 5 mg L^{-1}. The spinel $ZnCo_2O_4$, prepared by co-precipitation from the nitrates precursors and characterized by photoelectrochemistry, gives a conduction band of − 1.49 V_{SCE}, more cathodic than the $HCrO_4^-$ level (0.53 V). Therefore, the photoelectrons transfer toward $HCrO_4^-$ species is achieved through TiO_2 located midway between the spinel and chromate levels. The photocatalysis is investigated by varying the catalyst dose and $HCrO_4^-$ concentration. ZnCo2O4 has a gap of 1.82 eV and the best reduction efficiency (82%) was obtained under visible light (50 mW cm^{-2}) and optimal conditions ($HCrO_4^-$ 23 mg L^{-1}, pH ~ 7, $ZnCo_2O_4/TiO_2$ 50/50%) and follows a first-order kinetic with a rate constant of 3.86×10^{-3} min^{-1}.

Keywords Date pits · Chemical and physical activation · Adsorption · Chromate · Photoreduction · Hetero-system $ZnCo_2O_4/TiO_2$

Introduction

In the water treatment for the potable water production, the adsorption on activated carbons remains an attractive challenge for the environmental protection. Activated carbon (AC) is composed of a substantially amorphous carbon material (Bansal et al. 1988; Bouchemal et al. 2012; Tawfik Saleh 2015), delivering highly porous texture, a large specific surface area, a good adsorption capacity and a thermal stability (Skodras et al. 2008; Li et al. 2013; Alswat et al. 2016). Recent developments in the physical adsorption have highlighted the applications of AC. In this regard, the adsorption of gases (Wang et al. 2012; Abiko et al. 2010; Balarak et al. 2017), the uptake of organophosphorus pollutants (Jayson et al. 1982), the retention of bacteriologic pollutants in aqueous electrolytes (Oya et al. 1993), the elimination of heavy metals (Lu et al. 2014; Gomez-Eyles et al. 2013) and chromate photoreduction (Dermèche et al. 2017) are mainly documented in the open literature. AC is also used in bleaching and deodorization of certain liquids and can further play a role as catalyst support in heterogeneous catalysis (Polcaro et al. 1993; Qi et al. 2012). As the water quality is more stringent by the World Health Organization, an increased interest was focused on adsorbents (Ghasemian et al. 2015),

Electronic supplementary material The online version of this article (https://doi.org/10.1007/s13201-018-0755-1) contains supplementary material, which is available to authorized users.

✉ G. Rekhila
rekhilagharib@gmail.com

[1] Laboratoire d'étude physico-chimique des matériaux et application à l'environnement, Faculté de Chimie, Université des sciences et de la technologie USTHB, Algiers, Algeria

[2] Centre de Recherche scientifique et technique en Analyse Physico-Chimiques, Tipaza, Algeria

[3] Laboratory of Storage and Valorization of Renewable Energies, Faculty of Chemistry, USTHB, P.O. Box 32, 16111 Algiers, Algeria

zeolites (Mekatel et al. 2015; Lemraski and Palizban 2015), clays (Boutra et al. 2017) and activated carbons (Belhamdi et al. 2016; Merzougui et al. 2011) which are widely summarized in review articles. The porosity of AC is crucial for the adsorption and remains improperly explored; it is developed after pyrolysis of the carbon precursor under inert atmosphere. Thus, the adsorption capacity is usually insufficient for the utilization to which it was designated and developing the porous texture of AC remains a priority goal. So, the first part of our work is devoted to the influence of chemical and physical activations using $ZnCl_2$ and CO_2 flow on the porous texture of AC obtained from Algerian dates pits. The elaboration of activated carbons is applied for the elimination of inorganic pollutants. In this respect, Cr(VI) is a hazardous compound, selected for the pollution tests, in aqueous media for the adsorption on AC. Chromate comes mainly from tanneries, plating and battery factories and gives rise to large-scale pollution. Therefore, the second part of the work aims at determining the water decontamination by photocatalysis (Saleh and Gupta 2012; Gupta et al. 2012). Indeed, the adsorption yield increases the abatement but becomes inefficient at low concentrations. At this level, the photocatalysis is a clean alternative for the water decontamination which reduces the chromate ions to less harmful forms (Cr^{3+}) by photoelectrons (Rekhila et al. 2016). In this regard, the semiconductors with medium forbidden band are promising for the exploitation of a large part of the solar energy (Rekhila et al. 2013). The study focuses on the $HCrO_4^-$ reduction under visible light on the hetero-system $ZnCo_2O_4/TiO_2$. The charge transfer occurs iso-energetically and TiO_2 acts a bridge between the conduction band (CB) of $ZnCo_2O_4$ and adsorbed $HCrO_4^-$ ions. Nano-crystallites produce larger active surface areas with more photoelectrochemical sites, and the spinel $ZnCo_2O_4$ was prepared by chemical route at lower temperatures. It was selected because of its low cost, light absorption in the visible region and environmentally friendly characteristics (Guo et al. 2014).

Experimental setup

Preparation of activated carbons (AC)

Date pits (origin Algeria) are used for the preparation of activated carbons AC. At first, the stones were thoroughly washed with distilled water and dried in an air oven at 120 °C; such protocol was effective to facilitate crushing and grinding. A fraction particle size of between 0.5 and 1 mm was used for the preparation of activated carbons. AC prepared by combining physical and chemical activations was referred in the text as DZCO2: The precursor was impregnated with 7.32 mmol of $ZnCl_2$ as chemical adjuvant in a solid form and then pyrolyzed at 800 °C (heating rate of 5 °C/min) under low N_2 flow, followed by physical activation (800 °C) under CO_2 flow (20 L h^{-1}, 1 h) and cooled to room temperature. The sample was treated by HCl solution (0.1 M) under reflux ebullition (150 °C, 3 h) in order to eliminate the alkaline compounds and adjuvant excess. DZCO2 was recovered by filtration and thoroughly washed with distilled boiling water until the $AgNO_3$ test on the filtrate became negative. Finally, DZCO2 was dried in air oven at 120 °C (24 h) and stored in glass bottles until use.

The specific surface area was determined with a Micrometrics ASAP 2010 equipment at 77 K. Before measurement, the powder was degassed under vacuum (150 °C, 12 h). The morphology of DZCO2 was studied by scanning electron microscopy (SEM) using a JEOL, JSM-6360LV microscope.

The $HCrO_4^-$ stock solution (1 g L^{-1}) was prepared by dissolving the accurate amount of $K_2Cr_2O_7$ (Merck, 99%) in distilled water. The solutions with initial concentrations C_o (30, 50, 70 and 100 mg L^{-1}) were made up by dilution. Batch adsorption tests were carried out in 100-mL Erlenmeyer flasks placed in a thermostat shaker bath at 25 °C for 2 days. The adsorption study was realized at natural solution without any pH adjustment in order to avoid the interferences.

The kinetic study was realized for the adsorption equilibrium according to the following protocol: 50 mg of DZCO2 samples immersed in 100 mL of $HCrO_4^-$ solutions with different concentrations C_o for predetermined time intervals. The solutions were separated from adsorbent by centrifugation (4000 rpm, 5 min), and the $HCrO_4^-$ concentration was analyzed with a UV–visible spectrophotometer (Jasco V-630); $HCrO_4^-$ absorbs at 348 nm ($\varepsilon = 1770$ cm^{-1} mol^{-1} L) (Charlot 1961). The absorbance calibration curves were plotted versus the concentration of $HCrO_4^-$. The sampling was performed every 15 min during the first hour and more spaced beyond 1 h. The adsorbed amount Q_t (µmol/g), at time t, was calculated from the relation:

$$Q_t = \frac{V}{m}(C_0 - C_t) \quad (1)$$

where C_t is the liquid concentration at time t, V the volume of the solution and m the mass of AC. The adsorption isotherms are useful for the knowledge of the adsorbate/adsorbent interactions, and several models for analyzing the adsorption equilibrium data exist.

The second part was devoted to the $HCrO_4^-$ reduction under visible light on the hetero-system $CoZn_2O_4/TiO_2$. The spinel $ZnCo_2O_4$ was prepared by co-precipitation; stoichiometric amounts of $Co(NO_3)_2{\cdot}5H_2O$ (purity 99%, Merck) and $Zn(NO_3)_2{\cdot}6H_2O$ (99%, Prolabo) were dissolved in distilled water. The solution was evaporated on a hot plate and heated at 150 °C for the nitrate decomposition until disappearance of brown NO_x fumes. Then, the

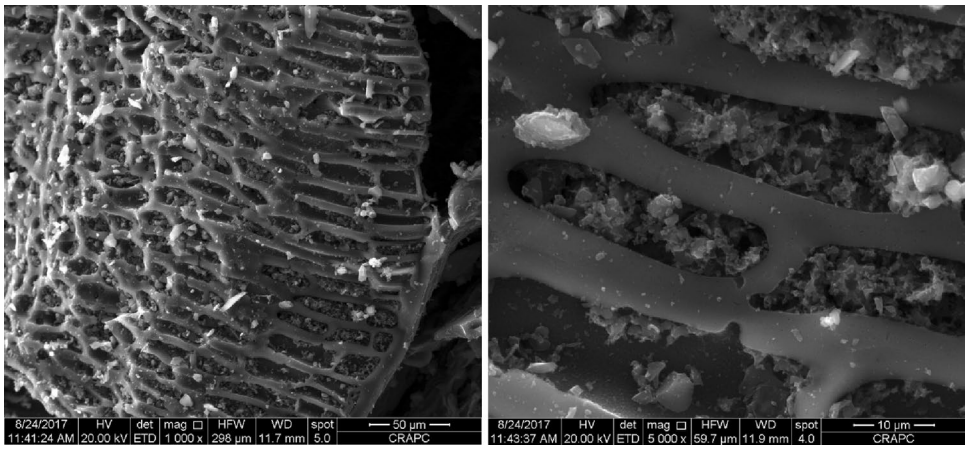

Fig. 1 SEM image of DZCO2 activated chemically with $ZnCl_2$ and pyrolyzed at 800 °C, then physically by CO_2

powder was ground in an agate mortar and reheated in a programmed furnace at 650 °C (10 °C min^{-1}, 16 h) with three intermediate regrindings. TiO_2 (99%) was supplied by Merck company. The phases were identified by X-ray diffraction (XRD) with a Mini-Diffractometer MD-10 using Cu K_α anticathode ($\lambda = 0.15418$ nm).

The forbidden band (E_g) was determined from the diffuse reflectance using a dual-beam spectrophotometer (Specord 200 Plus), and PTFE was used as standard. The point of zero charge (pzc) was simply obtained from the equilibrium pH of aqueous solution containing an excess of TiO_2 powder using a digital pH meter (Schott CG 825).

The photoelectrochemical (PEC) study was performed in a conventional cell using Pt as auxiliary electrode. The electrical contact on the back pellet was made with silver paint. The electrode surface of the pellet sintered at 700 °C was polished with emery paper (grade 80). The potential of $ZnCo_2O_4$ was monitored by PGZ301 potentiostat (Radiometer analytical) and given against a saturated calomel electrode (SCE). The Mott–Schottky characteristic was plotted at a frequency 10 kHz.

The photocatalytic device was composed by a Pyrex reactor open to atmosphere; the temperature was fixed at 25 °C thanks to a thermostated bath. The catalyst powder (100 mg) was suspended in 100 mL of $HCrO_4^-$ solution at different concentrations (8, 23, 32.5 and 43.5 mg L^{-1}) at natural pH (~ 7). The Erlenmeyers were maintained in the dark overnight and then exposed to visible light under magnetic agitation (400 rpm); the light intensity (mW cm^{-2}) was measured by a flux meter, and the concentration was determined as above.

Results and discussion

Characterization of activated carbons (DZCO2)

Textural characterization

The textural characteristics of DZCO2 gave a specific surface area of 1192 m^2 g^{-1} from the BET method through the N_2 adsorption isotherms. The mesoporous (V_{meso}, $\varnothing = 3.7$–50 nm), macroporous (V_{macro}, $\varnothing > 50$ nm) and microporous volumes (V_{micro}, $\varnothing < 3.7$ nm) were obtained from mercury intrusion porosimetry. The elemental analysis of the spinel confirmed the presence of Zn, Co and O. The crystallite size of $ZnCo_2O_4$ ($L \sim 45$ nm) was evaluated from the full width at half maximum (FWHM).

The microstructure of DZCO2 produced from date pits was examined by SEM images. Figure 1 shows a rough surface with narrow cavities; this property is characteristic of lignocellulosic material indicating that the structure of the precursor is preserved after pyrolysis. The external morphology of DZCO2 shows homogeneous cavities on the surface, resulting from the evaporation of the chemical adjuvant during the chemical activation (up to 800 °C), followed by the physical activation under CO_2 flow. The combined activations liberate the occupied spaces and increase the specific surface area. These results prompted us to test our sample for the adsorption of inorganic pollutant, and hexavalent chromate was selected for the tests.

Adsorption of chromate under static conditions on AC

The adsorption processes from aqueous solutions of $K_2Cr_2O_7$ on DZCO2 were carried out at 25 °C. The

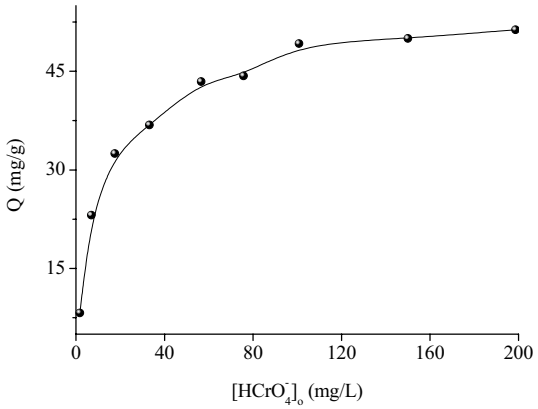

Fig. 2 Adsorption isotherm of $HCrO_4^-$ on DZCO2

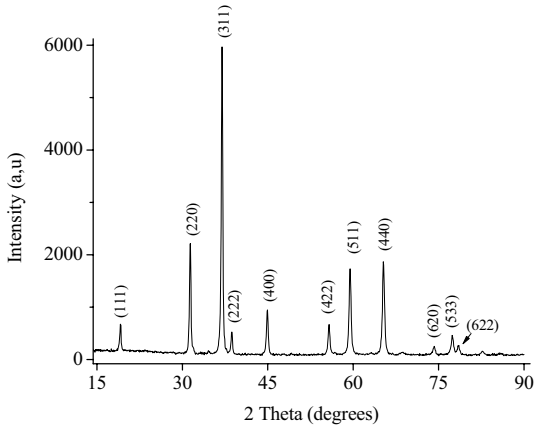

Fig. 3 The powder XRD pattern of $ZnCo_2O_4$ prepared by sol–gel and calcined at 650 °C

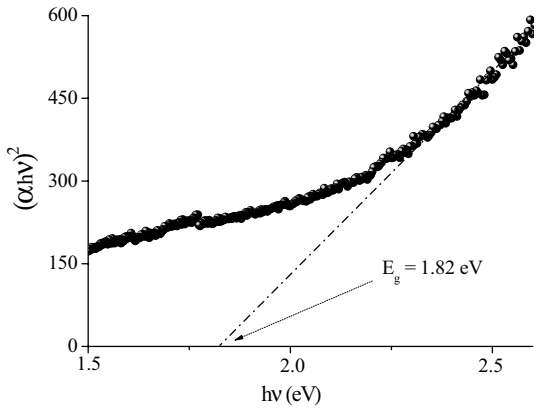

Fig. 4 The variation of $(\alpha h\nu)^2$ versus $h\nu$

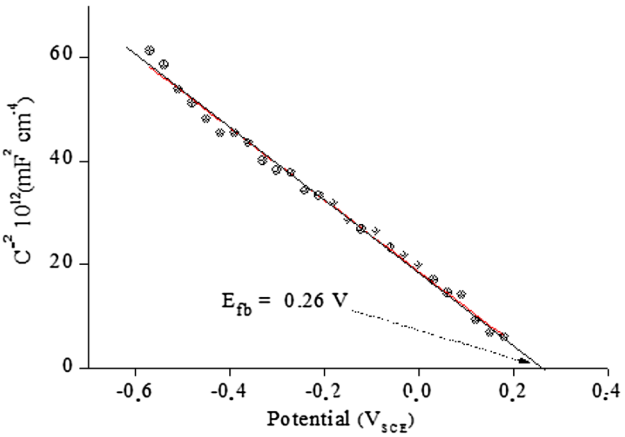

Fig. 5 The Mott–Schottky plot of *p*-type $ZnCo_2O_4$ in neutral solution (pH ~ 7)

behavior of DZCO2 obtained by chemical/physical activations was not identical; the volume V_{micro} increases with raising temperature and reaches a value of 0.63 $cm^3\ g^{-1}$ at 800 °C. DZCO2 has attractive properties for the $HCrO_4^-$ adsorption which shows a good performance; the adsorption isotherm (Fig. 2) is of L-type according to the Giles classification. To exploit the results, we have determined the maximum adsorption ($Q_{max} = 46.72$ mg/g) and the Langmuir constant ($K_L = 0.12$ L g^{-1}, SM1) from the linearized adsorption isotherms which depend on both the porous texture and chemical nature of the surface. It is worth noting that this value is close to those given in the literature (SM2). At pH ~ 7, the species $HCrO_4^-$ predominates and the small Q_{max} value is presumably due to the negative charge of chromate which is repelled by the negatively charged sites of DZCO2.

Photocatalysis

Chromate remains toxic even at low concentrations, and its presence in water is strongly regulated because it is highly hazardous and presents risks for the human health. The maximum limit was set up at 0.5 mg L^{-1} by the World Health Organization. The environmental photoelectrochemistry is an emerging technology, highly recommended for the pollution abatement (Omeiri et al. 2008). According to the standard powder diffraction data (JPCDS No 00-023-1390), the XRD pattern is characteristic of single phase of the normal spinel $Zn[Co]_2O_4$ (Fig. 3) (Yuanyuan et al. 2017; Venkatachalam et al. 2017). The optical gap (E_g) of the $ZnCo_2O_4$ is determined from the plot $(\alpha h\nu)^2$ versus the incident photon ($h\nu$) (Fig. 4)

$$(\alpha h\nu)^2 = \text{const} \times (h\nu - E_g) \quad (2)$$

where α is the absorption coefficient. The intersection with the $h\nu$-axis gives a direct gap of 1.82 eV, due to *d–d*

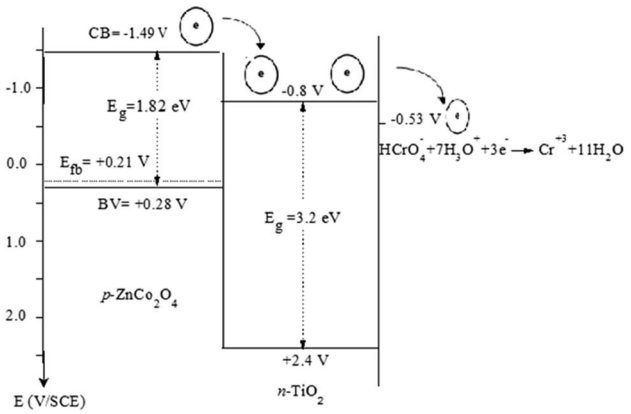

Fig. 6 The energy band diagram of $ZnCo_2O_4/TiO_2$/electrolyte junction of the photoelectrochemical cell

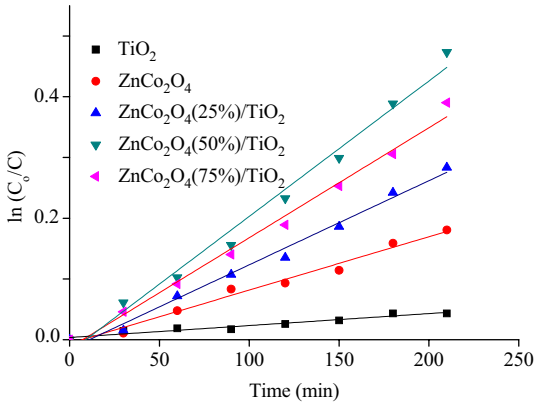

Fig. 7 The photocatalytic evolution of $HCrO_4^-$ reduction (8 mg L^{-1}) for various catalyst doses

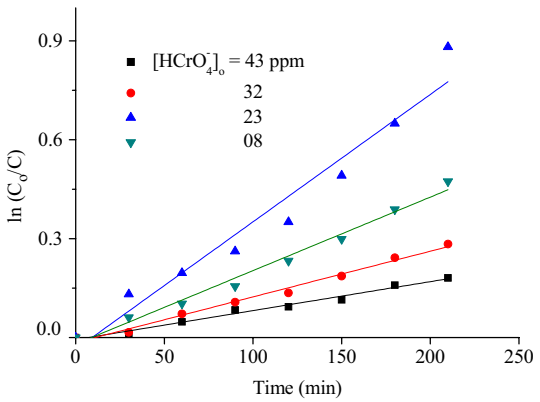

Fig. 8 The first-order kinetic model of $ZnCo_2O_4/TiO_2$ hetero-system for the $HCrO_4^-$ reduction for various initial concentration

transition coming from the crystal field splitting of Co^{3+} in octahedral coordination ($t_{2g}^3 e_g^2$).

The flat band potential (E_{fb}) is crucial in photocatalysis, and its value (+0.26 V) is reliably obtained from the capacitance versus applied potential, by extrapolation of the linear part to the abscissa axis (C^{-2}=0) (Fig. 5):

$$C^{-2} = (0.5 \times e\varepsilon\varepsilon_0 N_A)^{-1}\{E - E_{fb}\} \quad (3)$$

where N_A is the holes concentration and ε the permittivity of $ZnCo_2O_4$. The negative slope characterizes p-type conduction for $ZnCo_2O_4$ where the holes are the majority carriers. The potential of the conduction band (− 1.49 V = $E_{fb} - E_g/e + E_a/e$)[1] is negative enough to reduce $HCrO_4^-$ into trivalent state (~ −0.53 V) (Fig. 6).

The charge transfer in heterogeneous system occurs between levels of similar energy, and TiO_2 is used to mediate the electrons transfer since its conduction band is located midway between $ZnCo_2O_4$-CB and $HCrO_4^-$. Coupled semiconductors improve the separation of (e^-/h^+) pairs by synergetic effect and shift the spectral photoresponse toward longer wavelengths. Nano-crystallites of $ZnCo_2O_4$ prepared by chemical route give large active surface areas and more photocatalytic sites. $ZnCo_2O_4$ was chosen because of its light absorption over the visible region and chemical stability.

The sun spectrum overlaps the band gap of $ZnCo_2O_4$, and the reaction is kinetically governed by the electron flow in the sensitizer $ZnCo_2O_4$ because of the small diffusion length; therefore, nano-crystallites are attractive in such a case. The reduction in $HCrO_4^-$ is non-spontaneous, and the solar energy is used for it reduction to less harmful valence; Cr^{3+} is less hazardous and can be easily adsorbed. Moreover, the free potential of p-$ZnCo_2O_4$ is more negative than the flat band potential (− 1.49 V), yielding a spontaneous reduction under illumination. The photoelectrons located in $ZnCo_2O_4$-CB (− 1.49 V) are injected into TiO_2-CB (− 0.8 V) and subsequently transferred to $HCrO_4^-$ species (Fig. 6):

$$HCrO_4^- + 7H^+ + 3e^- \rightarrow Cr^{3+} + 4H_2O \quad \left(E^\circ \sim 0.53\ V\right) \quad (4)$$

The effect of the $ZnCo_2O_4$ dose in the hetero-system $ZnCo_2O_4/TiO_2$ on the photocatalytic process was studied, and the maximal efficiency is obtained for a mass ratio (50/50%) (Fig. 7). At low doses; the number of incident photons is larger than that of the photoelectrochemical sites and the photoactivity increases with raising the $ZnCo_2O_4$ mass. Conversely, for higher doses, the performance decreases because the catalyst works as optical filter and reduces the light penetration; the light scattering and shadowing effect also account for the decreased performance.

The chromate concentrations in industrial effluents can reach 50 mg L^{-1} and the influence of the remaining

[1] The activation energy (E_a ~ 0.07 eV) was determined from the electrical conductivity measurement on sintered pellet.

$HCrO_4^-$ concentration (C_o') is investigated in the range (8–43.5 mg L^{-1}) (Fig. 8). The color of the solution weakens over time and turns to white, an evidence of chromate disappearance. The reduction in $HCrO_4^-$ decreases when C_o' increases, because of the limited number of photocatalytic sites on the spinel surface. The photons flux is fixed, thus keeping constant the number of photoelectrons; so the increase in C_o' slows down the reduction because the remaining sites become less accessible due the inside porosity of $ZnCo_2O_4$ and repulsive forces between the $HCrO_4^-$ ions and the catalyst bulk.

Conclusion

This paper has given an overview on the preparation, characterization and application of adsorbent material based on activated carbon from date pits for the treatment of water polluted by chromate. We emphasized that the development of the porous texture of the activated carbon prepared by combined activations depends mainly on the nature of the adjuvant. The $HCrO_4^-$ adsorption of chromate on prepared adsorbent was carried out in a batch reactor, and the data were well filled by the Langmuir isotherm, while the adsorption kinetic followed a pseudo-first-order model. The remaining concentrations remain above the thresholds required by the water standard. Accordingly, the photoelectrochemical $HCrO_4^-$ reduction is reported on the heterosystem $ZnCo_2O_4/TiO_2$ to lower the concentration. The decay in the $HCrO_4^-$ absorbance is attributed to visible light reduction since no change was observed in the dark. The photocatalysis was optimized with respect to the $ZnCo_2O_4$ dose and $HCrO_4^-$ concentration, and a conversion of 82% was obtained.

References

Abiko H, Furuse M, Takano T (2010) Quantitative evaluation of the effect of moisture contents of coconut shell activated carbon used for respirators on adsorption capacity for organic vapors. Ind Health 48:52

Alswat AA, Bin Ahmad M, Saleh TA (2016) Zeolite modified with copper oxide and iron oxide for lead and arsenic adsorption from aqueous solutions. J Water Supply Res Technol AQUA 65:465–479

Balarak D, Mostafapour F, Bazrafshan E, Saleh TA (2017) Studies on the adsorption of amoxicillin on multi-wall carbon nanotubes. Water Sci Technol 75:1599–1606

Bansal RC, Donnet JB, Stoeckli F (1988) Active carbon. Marcel Dekker, New York

Belhamdi B, Merzougui Z, Trari M, Addoun A (2016) A kinetic, equilibrium and thermodynamic study of L-phenylalanine adsorption using activated carbon based on agricultural waste (date stones). J Appl Res Technol 14(5):354–366

Bihi N, Bennani-Ziatni M, Taitai A, Lebugle A (2002) Adsorption d'acides aminés sur des phosphates de calcium carbonatés analogues aux tissus calcifiés. Annales de Chimie Science des Matériaux 27:61–70

Bouchemal N, Azoudj Y, Merzougui Z, Addoun F (2012) Adsorption modeling of Orange G dye on mesoporous activated carbon prepared from Algerian date pits using experimental designs. Desalin Water Treat 45:284–290

Boutra B, Trari M, Nassrallah N, Bellal B (2017) Adsorption and photodegradation of solophenyl red 3BL on nanosized ZnFe2O4 under solar light. Theoret Exp Chem 197:490–497

Charlot G (1961) Les Méthodes de la chimie analytique: analyse quantitative minérale. Masson, Paris

Clark HM, Alves CC, Franca AS, Oliveira LS (2012) Evaluation of the performance of an agricultural residue-based activated carbon aiming at removal of phenylalanine from aqueous solutions. LWT-Food Sci Technol 49:155–161

Dermèche L, Rabia C, Rekhila G, Trari M (2017) Preparation and characterization of mixed caesium-tin mixed salt of Keggin-type phosphovanadomolybdate. Application to photocatalytic chromate reduction. Sol Energy Mater Sol Cells 168:45–50

Ghasemian M, Najafian Ashrafi Z, Goharkhah M, Ashjaee M (2015) Heat transfer characteristics of Fe_3O_4 ferrofluid flowing in a mini channel under constant and alternating magnetic fields. J Magn Magn Mater 381:158–167

Gomez-Eyles JL, Yupanqui C, Beckingham B, Riedel G, Gilmour C, Ghosh U (2013) Evaluation of biochars and activated carbons for in situ remediation of sediments impacted with organics, mercury, and methylmercury. Environ Sci Technol 47:13721

Guo H, Chen J, Weng W, Wang Q, Li S (2014) Facile template-free one-pot fabrication of ZnCo2O4 microspheres with enhanced photocatalytic activities under visible-light illumination. Chem Eng J 239:192–199

Gupta VK, Jain R, Mittal A, Saleh TA, Nayak A, Agarwal S, Sikarwar S (2012) Photo-catalytic degradation of toxic dye amaranth on TiO2/UV in aqueous suspensions. Mater Sci Eng C 32:12–17

Jayson GG, Lawless TA, Farihust D (1982) The adsorption of organic and inorganic phosphates onto a new activated carbon adsorbent. J Coll Inter Sci 86:379

Lemraski EG, Palizban Z (2015) Comparison of 2-amino benzyl alcohol adsorption onto activated carbon, silicon carbide nanoparticle and silicon carbide nanoparticle loaded on activated carbon. J Mol Liq 212:245–258

Li ZJ, Shi BY, Wang DS (2013) Comparative study on adsorption behaviors of natural organic matter by powered activated carbons with different particle sizes. Huan Jing Ke Xue 34:4319

Lu X, Jiang J, Sun K, Wang J, Zhang Y (2014) Influence of the pore structure and surface chemical properties of activated carbon on the adsorption of mercury from aqueous solutions. Mar Pollut Bull 78:69

Mekatel E, Amokrane S, Aid A, Nibou D, Trari M (2015) Adsorption of methyl orange on nanoparticles of a synthetic zeolite NaA/CuO. C R Chim 18(3):336–344

Merzougui Z, Azoudj Y, Bouchemel N, Addoun F (2011) Effect of activation method on the pore structure of activated carbon from date pits application to the treatment of water. Desalin Water Treat 29:236–240

Omeiri S, Gabès Y, Bouguelia A, Trari M (2008) Photoelectrochemical characterization of the delafossite $CuFeO_2$: application to removal of divalent metals ions. J Electroanal Chem 614(1–2):31–40

Oya A, Yoshida S, Abe Y, Lizuka T, Makiyama N (1993) Preparation of pitch-based antibacterial activated carbon fiber. Carbon 31:77

Polcaro AM, Palmas S, Dernini S (1993) Role of catalyst characteristics in electrocatalytic hydrogenation: reduction of benzaldehyde and acetophenone on carbon Felt/Pd electrodes. Ind Eng Chem Res 32:1315

Qi X, Guo H, Li L, Smith RL Jr (2012) Acid-catalyzed dehydration of fructose into 5-hydroxymethylfurfural by cellulose-derived amorphous carbon. Chem Sus Chem 5:2215

Rekhila G, Bessekhouad Y, Trari M (2013) Visible light hydrogen production on the novel ferrite NiFe2O4. Int J Hydrogen Energy 38(15):6335–6343

Rekhila G, Bessekhouad Y, Trari M (2016) Synthesis and characterization of the spinel $ZnFe_2O_4$, application to the chromate reduction under visible light. Environ Technol Innov 5:127–135

Saleh TA (2015) Mercury sorption by silica/carbon nanotubes and silica/activated carbon: a comparison study. J Water Supply Res Technol AQUA 64:892–903

Saleh TA, Gupta VK (2012) Photo-catalyzed degradation of hazardous dye methyl orange by use of a composite catalyst consisting of multi-walled carbon nanotubes and titanium dioxide. J Colloid Interface Sci 371:101–106

Skodras G, Diamantopoulou I, Pantoleontos G, Sakellaropoulos GP (2008) Kinetic studies of elemental mercury adsorption in activated carbon fixed bed reactor. J Hazard Mater 158:1

Venkatachalam V, Alsalme A, Alswieleh A, Jayavel R (2017) Double hydroxide mediated synthesis of nanostructured $ZnCo_2O_4$ as high performance electrode material for supercapacitor applications. Chem Eng J 321:474–483

Wang H, Jahandar Lashaki M, Fayaz M, Hashisho Z, Philips JH, Anderson JE, Nichols M (2012) Adsorption and desorption of mixtures of organic vapors on beaded activated carbon. Environ Sci Technol 46:8341

Yuanyuan P, Tian S, Yansong X, Linghao G, Liangyu S, HuijuanL G, Dong F (2017) Self-assembled hierarchical peony-like $ZnCo_2O_4$ for high-performance asymmetric supercapacitors. Electrochim Acta 253:281–290